7.6

SIMPLE FRONTAL MODELS OF BAROCLINIC INSTABILITY

Mateusz K. Reszka[1*], Gordon E. Swaters[2]
[1]University of Toronto, Toronto, Canada
[2]University of Alberta, Edmonton, Canada

1. INTRODUCTION

Density-driven currents, characterized by a balance between the pressure gradient and the Coriolis force, are often associated with sharp horizontal and vertical density gradients that separate water masses with different physical, chemical and biological properties. Distinct, relatively fast-flowing currents may be found at all depths in the ocean, and are known to undergo vigorous baroclinic (and barotropic) instabilities, which give rise to eddies and enhance mixing (e.g. Rhines 1977).

We present recent results concerning two models for baroclinic instability. Both models have the configuration of a two-layer fluid, with one baroclinic (frontal) layer and one relatively-deep (ambient) layer. The layer interface serves as an efficient, though idealized, representation of a steep density gradient. Although we will make a number of simplifying assumptions, we will require that the models allow for varying topography and vanishing thickness of the frontal layer. The latter assumption precludes the use of the quasigeostrophic (QG) formalism, in which only small displacements of the interface are allowed. We focus on the effects of topography and ambient stratification on linear stability. These models have been used in the past to investigate aspects of instability associated with the California Current system and the Denmark Strait overflow (Reszka 2003).

2. GENERAL MODEL FEATURES

Here we describe features common to both models. In the baroclinic layer, a fully nonlinear mass conservation equation will be retained, however leading-order geostrophy will still be assumed in both layers. In this case, a small Rossby number, ε, results not from the requirement of small velocities, as in QG theory, but from the condition that the dynamic lengthscale L is much larger than the internal deformation radius R. Since geostrophic balance (e.g. in shallow water theory) implies $\varepsilon = (R/L)^2$, we only require that $L^2 \gg R^2$, not $L \gg R$. Consequently (adopting the notion that a factor of 10 corresponds to an "order of magnitude") flows for which $L > \sqrt{10}R$ may already fall in this regime (Cushman-Roisin 1986).

The frontal layer is assumed to be homogeneous and its scale thickness, as well as topographic variations, are both assumed small compared to the total fluid depth H. The ambient layer is in hydrostatic balance and includes a z-dependent background density as well as a space/time-dependent density fluctuation. The lengthscale is taken to be greater than the deformation radius of the baroclinic layer and time is scaled advectively with the ambient fluid. Surface and internal gravity wave modes are filtered out by the rigid lid approximation and a subinertial scaling of the velocities. Finally, vertical velocity is assumed to scale as the time derivative of the frontal layer thickness.

3. SURFACE CURRENTS

3.1 *Governing Equations*

The equations derived here are a novel generalization of a previous frontal geostrophic model for buoyancy-driven surface currents (Cushman-Roisin *et al.* 1992; Swaters 1993). The scalings employed are the same as in Swaters (1993), modified however, to allow stratification of the lower layer. A detailed development, including a discussion of source/sink terms and the beta effect may be found in Reszka (2003). A diagram of the prototypical model configuration is given in Figure 1.

A straightforward way to obtain the governing set is to first introduce the above assumptions into the shallow water equations for the frontal (i.e. upper) layer and the Boussinesq system for the ambient (i.e. lower) layer. Expanding all flow variables in the Rossby number, it will turn out that the leading order problem associated with the upper layer mass conservation equation is trivial. At the next order, velocity corrections from the advective terms in the momentum equation will enter the balance, leading to a frontal geostrophic (Cushman-Roisin 1986) evolution equation for the upper layer thickness h. Our govern-

*Corresponding author address: Dept. of Physics, University of Toronto, 60 St. George Street, Toronto, Ontario, M5S 1A7, Canada; *E-mail*: matt@atmosp.physics.utoronto.ca

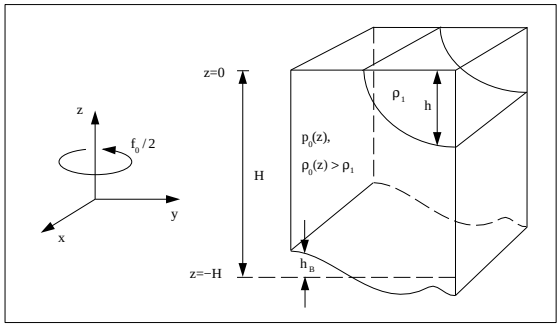

Figure 1: Model geometry. A thin, homogeneous layer overlies a continuously-stratified layer that is relatively deep, but finite. The fluid interface is allowed to intersect the surface, thus forming true fronts. The topography may be flat or spatially varying.

ing equations on an f-plane can be written as follows,

$$h_t + J(\varphi + h\Delta h + \tfrac{1}{2}\nabla h\cdot\nabla h, h) = 0, \qquad z = 0, \quad (1)$$

$$\varphi_{zt} + J(\varphi, \varphi_z) + BJ(h\Delta h + \tfrac{1}{2}\nabla h\cdot\nabla h, h) = 0, \qquad z = 0, \quad (2)$$

$$(\Delta\varphi + (\frac{1}{B}\varphi_z)_z)_t + J(\varphi, \Delta\varphi + (\frac{1}{B}\varphi_z)_z) = 0, \quad (3)$$

$$\varphi_{zt} + J(\varphi, \varphi_z) + BJ(\varphi, h_B) = 0, \qquad z = -1, \quad (4)$$

with the auxiliary relations

$$\mathbf{u}_1 = \mathbf{e}_3 \times \nabla h, \qquad \mathbf{u}_2 = \mathbf{e}_3 \times \nabla\varphi,$$

$$w = -\frac{1}{B}[\varphi_{zt} + J(\varphi, \varphi_z)], \qquad \rho = -\varphi_z. \quad (5)$$

Here $\varphi(x, y, z, t)$, $\mathbf{u}_1(x, y, t)$, $\mathbf{u}_2(x, y, z, t)$, $w(x, y, z, t)$ and $\rho(x, y, z, t)$ are the upper layer geostrophic pressure, upper and lower layer horizontal velocities, lower layer vertical velocity and lower layer density fluctuation, respectively. Also, $h_B(x, y)$ is the topographic height, $\Delta = \nabla\cdot\nabla$, $J(a, b) = a_x b_y - a_y b_x$ and $B(z)$ is the Burger number,

$$B \equiv \frac{N^2(z)H^2}{f_0^2 L^2}, \quad (6)$$

for the lower layer.

The upper layer thickness $h(x, y, t)$ is advected by the lower layer streamfunction and also by velocity corrections represented by the cubic nonlinearities in (1). The lower layer is governed by QG dynamics for a continuously stratified fluid (3) with no-normal-flow conditions applied at the top (2) and bottom (4) of the layer. The baroclinic coupling of the layers is between equations (1) and (2). The above system reduces to that of Cushman-Roisin *et al.*(1992) and Swaters (1993) in the limit $B \to 0$ (Reszka 2003).

3.2 *Linear Results*

We wish to investigate the effect of infinitesimal perturbations to a steady mean flow. For simplicity, we will assume constant stratification $B = $ const., linearly sloping topography $h_B = \nu y$ and an x-periodic channel domain with $0 < y < y_{\max}$. We consider the steady reference state $(h = h_0(y), \varphi = 0)$, where h vanishes along at most one x-periodic curve $y = \xi(x, t)$. Normal mode solutions of the form

$$\begin{bmatrix}\varphi\\ h\\ \xi\end{bmatrix} = \begin{bmatrix}0\\ h_0(y)\\ b\end{bmatrix} + \begin{bmatrix}\tilde\varphi(y, z)\\ \tilde h(y)\\ \tilde\xi\end{bmatrix} e^{ik(x-ct)} + \text{c.c.}, \quad (7)$$

are assumed, where $0 \le b < y_{\max}$ is the initial location of the frontal outcropping, k is the along-channel wavenumber, c is the complex phase speed and c.c. refers to the complex conjugate. Dropping the tildes, the linearized equations become

$$\varphi_{yy} + \frac{1}{B}\varphi_{zz} - k^2\varphi = 0, \quad (8)$$

$$\left.\begin{aligned} h_{0y}\varphi - \mathcal{L}[h] &= ch,\\ -B\mathcal{L}[h] &= c\varphi_z,\end{aligned}\right\} z = 0, \quad (9)$$

$$\nu B\varphi = c\varphi_z, \qquad z = -1, \quad (10)$$

where the operator $\mathcal{L}$ is defined by

$$\mathcal{L}[*] = \{(h_0 h_{0yy})_y + h_0 h_{0y}(k^2 - \partial_{yy}) - h_{0y}^2\partial_y\}[*]. \quad (11)$$

Now ξ is determined diagnostically from

$$\xi = -\frac{h}{h_{0y}} \qquad y = b. \quad (12)$$

No normal-flow at the channel walls also implies

$$h, \varphi = 0 \qquad y = 0, y_{\max}. \quad (13)$$

The energy equation associated with (8)–(10) provides a stability condition analogous to that found in Swaters (1993). Defining, for notational convenience, $s = -\nu$ and $\alpha = \max(h_{0y})$, a sufficient condition for stability is

$$0 < \alpha < s\frac{\int_0^{y_{\max}} |\varphi|^2_{z=-1}\ dy}{\int_0^{y_{\max}} |\varphi|^2_{z=0}\ dy}, \quad (14)$$

(Reszka 2003). Thus, sufficiently steep topography stabilizes the flow, if the topographic and interfacial slope have the same sign. However, for surface-intensified flows, the ratio of integrals in (14) will typically be less than unity, thus implying a smaller region of stability than the corresponding homogeneous stability condition (Swaters 1993)

$$0 < \alpha < s. \quad (15)$$

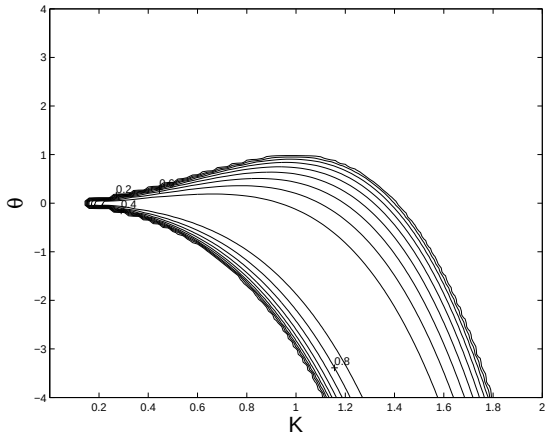

Figure 2: Imaginary part of the phase speed, c_I, as a function of the horizontal wavenumber K and the ratio of bottom slope to frontal slope, $\theta = s/\alpha$, for a homogeneous lower layer (limit as $B \to 0$). All instability is suppressed for $\theta > 1$.

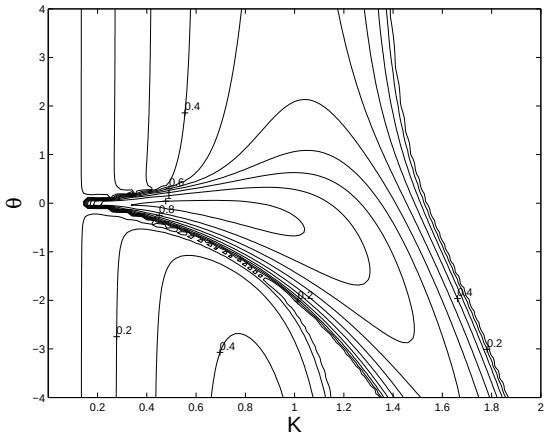

Figure 3: Same as Figure 2 but for a continuously-stratifi ed lower layer with $B = 0.5$. The unstable region is larger than in the $B = 0$ case, and a second mode of instability appears at low wavenumbers for $\theta < 0$.

Separated solutions to the normal mode problem may easily be found for the case of a gently sloping wedge front, $h_0 = 1 + \alpha y$, where $\alpha = O(\nu) \ll 1$. Although this linearly sloping profile does not actually vanish, it provides insight into the stability properties of the system. Retaining only $O(1)$ terms, while keeping in mind that c will also turn out to be $O(\alpha)$, solutions may be sought in the form

$$h_n = a_n \sin(l_n y), \tag{16}$$

$$\varphi_n = \sin(l_n y) \times [b_n \cosh(\lambda_n (z+1)) + c_n \cosh(\lambda_n z)], \tag{17}$$

with unknown coefficients a_n, b_n and c_n, where

$$l_n = \frac{n\pi}{y_{\max}}, \quad K_n = \sqrt{k^2 + l_n^2}, \quad \lambda_n = \sqrt{B} K_n, \tag{18}$$

are the cross-channel, horizontal and vertical wavenumbers, respectively, for $n = 1, 2, 3, \ldots$ After substitution into (8)–(10) the dispersion relation is obtained by requiring that the determinant of the coefficient matrix vanishes. Introducing the notation $T_n = \tanh(\lambda_n)/\lambda_n$, we thus obtain the cubic equation (Reszka 2003),

$$(\lambda_n^2 T_n) c^3 + B(\alpha K_n^4 T_n + \nu) c^2 + \alpha \lambda_n^2 (\alpha + \nu) c + \alpha^2 \nu B \lambda_n^2 T_n = 0. \tag{19}$$

Since the gravest cross-channel mode will be dominant, henceforth we fix $n = 1$ and drop the subscript n. For a channel width of 10.0, (18) also fixes l. In Figure 2 we plot c_I, the imaginary part of the phase speed, as a function of K and the slope ratio $\theta = s/\alpha$, in the limiting case of no stratification in the lower layer. Surfaces of the growth rate, $\sigma = kc_I$ are qualitatively similar. Clearly, growth is suppressed whenever (15) is satisfied.

However, this no longer holds when the lower layer is stratified. Figure 3 is a plot of c_I versus K and θ for $B = 0.5$, i.e. a moderate value of the Burger number. First of all, growth rates are no longer zero for $s > \alpha$. Indeed, unstable wavenumbers can be found for all slope ratios shown. Also, a second mode of instability has appeared for low values of K and negative θ (i.e. topographic and interfacial slopes are of opposite sign). Indeed, the spatial structure of the perturbation solution (not shown) consists of both a surface- and bottom-intensified mode.

The interplay of topography and frontal slope can be appreciated further by examining the maximum growth rate (over k) in $\alpha - s$ space. For $B = 0$ (Figure 4), growth rates increase with α, decrease with s, and vanish for $s > \alpha$, as we would expect. For $B = 0.5$ (Figure 5), the unstable region expands significantly. For fixed α, steep topography $s > 0$ is still a stabilizing influence in the sense that growth rates are decreased as s increases. However they do not vanish, as they do in the homogeneous case.

Interestingly, Figure 5 also seems to suggest a weak stabilizing influence of the topography when α is small and $s < 0$. In other words, growth rates decrease somewhat as the topography steepens, even if it slopes in the opposite sense to the front, although this influence is much less pronounced than in the case $\alpha s > 0$. Thus, even in this highly idealized situation, the role of bottom topography is not trivial.

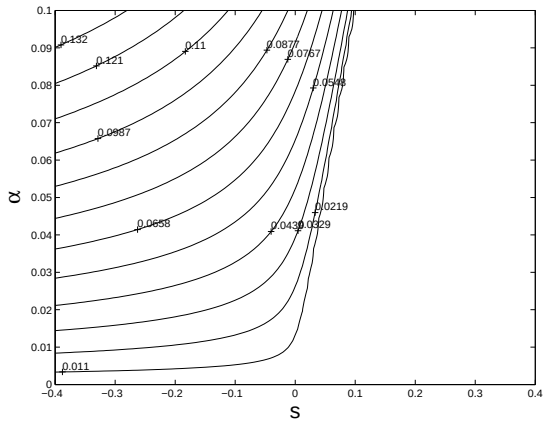

Figure 4: Maximum growth rate kc_I (over k) as a function of α and s for $B = 0$.

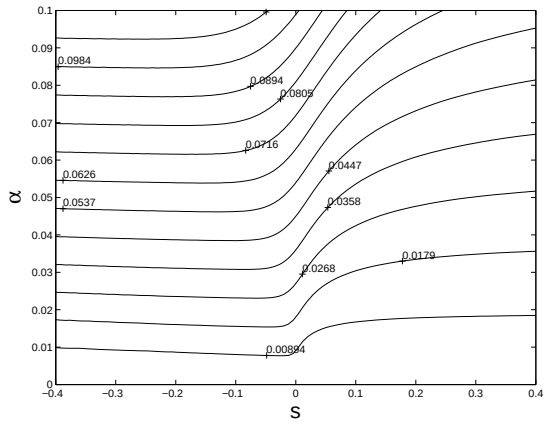

Figure 5: As Figure 4 but with $B = 0.5$.

4. BOTTOM-TRAPPED CURRENTS

4.1 *Governing Equations*

An analogous model may be derived for the description of terrain-following dense flows, where the baroclinic fluid now comprises the lower layer, and hugs the topography. A schematic of the model configuration is presented in Figure 6. A rigorous derivation of this model appears in Poulin and Swaters (1999), while the addition of sources, sinks and bottom drag is discussed in Reszka *et al.* (2002). Here, the governing equations are simply stated for completeness.

To leading order in the Rossby number we have

$$\varphi_{zt} + \mu J(\varphi, \varphi_z) = 0, \qquad z = 0, \tag{20}$$

$$(\Delta\varphi + (\frac{1}{B}\varphi_z)_z)_t + \mu J(\varphi, \Delta\varphi + (\frac{1}{B}\varphi_z)_z) = 0, \tag{21}$$

$$\varphi_{zt} + \mu J(\varphi, \varphi_z) + BJ(\varphi + h, h_B) = 0, \qquad z = -1, \tag{22}$$

$$h_t + J(\mu\varphi + h_B, h) = 0, \qquad z = -1. \tag{23}$$

The notation is similar to that used in the previous section, except that the roles of the two layers are, in a sense, reversed. An important difference is that the frontal layer velocity is now given by

$$\mathbf{u}_2 = \mathbf{e}_3 \times \nabla p, \tag{24}$$

where the lower-layer geostrophic pressure is defined to be

$$p = h_B + \mu(\varphi|_{z=-1} + h). \tag{25}$$

The parameter μ is the ratio of upper- to lower-layer Rossby number (and is assumed to be O(1)) but also measures the relative importance of baroclinicity versus topographic steepness. The coupling of equations (22) and (23) determines the baroclinic nature of the system as a whole.

The frontal evolution equation (23) represents the "planetary geostrophic" limit (deVerdière, 1981). Although the mass conservation equation is fully nonlinear, the only contribution from the momentum equations is geostrophic balance. It turns out that this dynamic regime arises naturally from the assumption that the upper layer pressure, frontal layer thickness and bottom topography contribute equally to the lower layer geostrophic pressure (25). This model serves to investigate the situation in which the bottom trapped current is topographically steered, density driven, and fully coupled with upper layer dynamics at leading order.

4.2 *Linear Results*

Perturbation solutions for a wedge front profile have been described by Poulin and Swaters (1999). Here we outline the solution of the linearized problem corresponding to a front that is concave-down in cross-section. We assume the basic state $(h = h_0(y), \varphi = 0)$, B constant, and $h_B = \nu y$ in an x-periodic channel with $-y_{\max} < y < y_{\max}$. A frontal profile that intersects the topography along two distinct curves, say $y = \xi_1(x,t)$, $y = \xi_2(x,t)$, is a reasonable approximation to a typical dense overflow after geostrophic adjustment (Meacham and Stephens, 2001).

Assuming normal mode solutions

$$\begin{bmatrix} \varphi \\ h \\ \xi_1 \\ \xi_2 \end{bmatrix} = \begin{bmatrix} 0 \\ h_0(y) \\ a_1 \\ a_2 \end{bmatrix} + \begin{bmatrix} \tilde{\varphi}(y,z) \\ \tilde{h}(y) \\ \tilde{\xi}_1 \\ \tilde{\xi}_2 \end{bmatrix} \mathrm{e}^{ik(x-ct)} + \text{c.c.}, \tag{26}$$

for constants $-y_{\max} \le a_1 < a_2 \le y_{\max}$, and dropping the tildes, the linearized problem has the form

$$-k^2\varphi + \varphi_{yy} + N^{-2}\varphi_{zz} = 0, \tag{27}$$

$$\varphi_z = 0, \qquad z = 0, \tag{28}$$

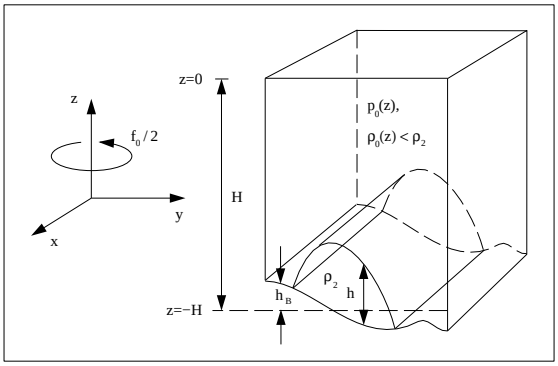

Figure 6: Model geometry. A deep but finite continuously-stratified layer overlies a relatively thin, homogeneous layer situated on sloping, or otherwise varying, topography. The interface is allowed to intersect the topography, forming true fronts.

$$\left.\begin{aligned} \varphi_z &= \nu B \frac{c+\mu h_{0y}+\nu}{c(c+\nu)}\varphi, \\ \mu h_{0y}\varphi - \nu h &= ch, \end{aligned}\right\} z=-1, \qquad (29)$$

where ξ_1, ξ_2 are determined diagnostically from

$$\xi_i = -\frac{\mu}{c+\nu}\varphi(a_i,-1), \qquad i=1,2. \qquad (30)$$

For a parabolic initial profile,

$$h_0(y) = \max[1-(y/a)^2, 0], \qquad (31)$$

we have $a_2 = -a_1 = a$ and, moreover, (27)–(29) is nonseparable. Defining

$$Y_n = \frac{n\pi(y+y_{\max})}{2y_{\max}}, \qquad (32)$$

we seek solutions of the form

$$\varphi(y,z) = \frac{1}{\sqrt{y_{\max}}}\sum_{n=1}^{\infty} b_n \sin Y_n \cosh(\lambda_n z), \qquad (33)$$

where the meaning of λ_n is similar to (18). The expansion coefficients b_n can be found numerically by solving the associated eigenvalue problem, after truncation at a finite number of expansion modes (Reszka *et al.* 2002). Below, we discuss the resulting instability characteristics for $y_{\max}=5.0$, $a=2.5$, $\nu=1.0$ and $B=1.0$.

Figure 7 shows the maximum growth rate as a function of the interaction parameter μ and Burger number B. Growth rates increase with both parameters, as does the dominant wavenumber (not shown). The dependence on μ (on B) becomes quasi-linear for large B (large μ). Here an increase in μ may be interpreted as an increase in the relative thickness of the

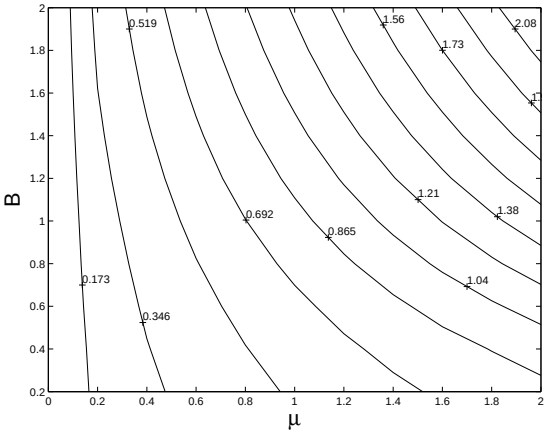

Figure 7: Maximum growth rate kc_I as a function of the interaction parameter μ and Burger number B, for a bottom trapped current with a parabolic profile. Growth rates increase with both μ and B. Here an increase in μ corresponds to a thicker lower layer.

lower layer (Poulin and Swaters 1999). Not surprisingly, a more baroclinic system yields a more vigorous instability. An increase in B also results in faster growth, since higher stratification reduces the "effective depth" of the upper layer (Lane-Serff and Baines 2000), again enhancing the baroclinic nature of the system.

The effect of topography is demonstrated in Figure 8. An assumption of the model derivation was that, for a fixed upper layer Rossby number, time and bottom slope scale with $1/\mu$ and μ, respectively. In order to appreciate the trend in dimensional growth rate, in Figure 8 we plot the maximum growth rate scaled by μ^{-1} in the $B-\mu^{-1}$ plane. Predicted numerical values for dimensional growth rates and dominant wavelengths relevant to the Denmark Strait overflow are discussed in Reszka *et* al. 2002. Here we note that increasing topographic slope is a destabilizing influence for frontal profiles such as (31).

5. Discussion

Instabilities in both of the above models rely on the release of available potential energy. In Section 3 the energy released is due to a gradual spreading of the front, and the process is completely baroclinic, in the sense that a (monotonic) front is stable in the absence of the lower layer (Swaters 1993). In Section 4, energy is provided by the flattening of the frontal profile and by the gradual descent of the dense fluid down the sloping topography. In fact, the second of these mechanisms is the dominant one (Reszka 2003). Be-

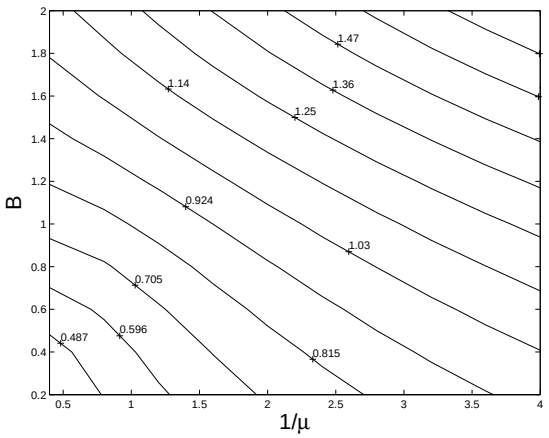

Figure 8: Scaled maximum growth rate kc_I/μ as a function of $1/\mu$ and B, for a bottom trapped current with a parabolic profi le. The trend in kc_I/μ represents the trend in the dimensional growth rate, where an increase in $1/\mu$ corresponds to steeper bottom topography.

cause of this strong influence of the topography, the planetary geostrophic approximation provides one of the few consistent scalings for bottom-trapped flows.

Stability conditions (14), (15) are analogous to that for a two-layer QG fluid (Pedlosky 1987), in the sense that the corresponding necessary condition for instability is satisfied if, for example, leading order cross-channel potential vorticity gradients are constant but of opposite sign in the two layers. However, the utility of the model (1)–(4) is in its applicability to situations in which QG theory (layered or continuously stratified) is inappropriate, either due to large lengthscales or vanishing fronts.

Linear stability criteria associated with (27)–(29) can also be related to those for a two-layer QG fluid, but with caution. For clarity, we focus on the limit $B = 0$ and, without loss of generality, assume that $h_{By} > 0$. The y-integrated energy equation yields a sufficient condition for stability,

$$h_{By} h_{0y} < 0 \qquad \text{for all } y, \tag{34}$$

(Poulin and Swaters 1999). If we define the absolute interfacial height as $h_A(y) \equiv h_B(y) + h_0(y)$, then the above criterion is equivalent to

$$h_{By} > h_{Ay} \qquad \text{for all } y. \tag{35}$$

If, in addition, $h_{Ay} h_{By} > 0$ then such a configuration is stable according to QG theory, since the leading order potential vorticity gradients in the upper and lower layers are h_{Ay} and $-h_{0y}/h_0^2$, respectively.

However, if $h_{Ay} h_{By} < 0$, flow satisfying (35) will still be stable, due to the prominent role of interfacial deformations in the model. Lower layer vorticity waves travel in the negative x-direction for $h_{0y} < 0$ and cannot couple with those in the upper layer, travelling in the positive x-direction for $h_{Ay} < 0$. Finally, we note that defining $h_A \equiv -h_0$ for the model in section 3, and assuming $h_{Ay} h_{By} > 0$, stability condition (15) also reduces to (35), which demonstrates a link in the stability properties of the two models, at least in this simple setting.

Acknowledgements. M.K.R. wishes to thank Prof. T. Shepherd for financial support in attending this AMS meeting.

REFERENCES

Cushman-Roisin, B., 1986: Frontal Geostrophic Dynamics. *J. Phys. Oceanogr.*, **22**, 117–127.

Cushman-Roisin, B., Sutyrin, G. G. and Tang, B., 1992: Two-layer Geostrophic Dynamics. Part I. Governing Equations. *J. Phys. Oceanogr.*, **20**, 758–768.

Lane-Serff, G. F. and Baines, P. G., 2000: Eddy Formation by Overflows in Stratified Water. *J. Phys. Oceanogr.*, **30**, 327-337.

Meacham, S. P. and Stephens, J. C., 2001: Instabilities of Gravitiy Currents along a Slope. *J. Phys. Oceanogr.*, **31**, 30–53.

Pedlosky, J., 1987: *Geophysical Fluid Dynamics* (2^{nd} ed.). New York. Springer. 710 pp.

Poulin, F. J. and Swaters, G. E., 1999: Sub-inertial dynamics of density-driven flows in a continuously stratified fluid on a sloping bottom. I. Model derivation and stability characteristics. *Proc. R. Soc. Lond. A*, **455**, 2281–2304.

Reszka, M. K., 2003: Baroclinic Frontal Dynamics in the Presence of Continuous Stratification and Topography. *Ph.D. Thesis.*, Univeristy of Alberta. 220 pp.

Reszka, M. K., Swaters, G. E. and Sutherland, B. R., 2002: Instability of abyssal currents in a continuously stratified ocean with bottom topography. *J. Phys. Oceanogr.*, **32**, 3528–3550.

Rhines, P. B., 1977: The Dynamics of Unsteady Currents. In *The Sea*, vol. 6. Wiley Interscience, NY. 189–318.

Swaters, G. E., 1993: On the baroclinic dynamics, hamiltonian formulation and general stability characteristics of density-driven currents and fronts over a sloping continental shelf. *Phil. Trans. R. Soc. Lond. A*, **345**, 295–325.

deVerdière, A. C., 1981: On Mean Flow Instabilities within the Planetary Geostrophic Equations. *J. Phys. Oceanogr.*, **16**, 1981–1984.